Canonical Homotopy Class Representative Using Hyperbolic Structure

Wei Zeng[1], Miao Jin[2], Feng Luo[3], Xianfeng David Gu[1]

[1]Department of Computer Science, Stony Brook University, Stony Brook, NY 11794, USA

[2]Center for Advanced Computer Studies, University of Louisiana at Lafayette, Lafayette, LA 70504, USA

[3]Department of Mathematics, Rutgers University, Piscataway, NJ 08854, USA

***Abstract*—Homotopy group plays a role in computational topology with a fundamental importance. Each homotopy equivalence class contains an infinite number of loops. Finding a canonical representative within a homotopy class will simplify many computational tasks in computational topology, such as loop homotopy detection, pants decomposition. Furthermore, the canonical representative can be used as the shape descriptor.**

This work introduces a rigorous and practical method to compute a unique representative for each homotopy class. The main strategy is to use hyperbolic structure, such that each homotopy class has a unique closed geodesic, which is the representative.

The following is the algorithm pipeline: for a given surface with negative Euler number, we apply hyperbolic Yamabe curvature flow to compute the unique Riemannian metric, which has constant negative one curvature everywhere and is conformal to the original metric. Then we compute the Fuchsian group generators of the surface on the hyperbolic space. For a given loop on the surface, we lift it to the universal covering space, to obtain the Fuchsian transformation corresponding to the homotopy class of the loop. The unique closed geodesic inside the homotopy class is the axis of the Fuchsian transformation, which is the canonical representative.

Theories and algorithms are explained thoroughly in details. Experimental results are reported to show the efficiency and efficacy of the algorithm. The unique homotopy class representative can be applied for homotopy detection and shape comparison.

***Keywords*—homotopy class, hyperbolic structure, hyperbolic Yamabe flow**

1. INTRODUCTION

Computational topological methods have been widely applied for computer graphics, geometric modeling, medical imaging and many engineering fields. One of the most important topological invariant is the fundamental group. Comparing to homology groups, fundamental group conveys more information, but also is much more difficult to compute. For examples, verifying two fundamental groups of 3-manifolds are isomorphic, finding the shortest representative of a loop in the fundamental group, are highly non-trivial. Geometry topology aims at solving topological problems by equipping the topological manifold with a geometric structure, which can greatly simplify the problem. For example, in order to prove the Poincaré conjecture, a Riemannian metric is assigned to the 3-manifold, by running Ricci flow, the metric converges to the canonical spherical metric. This proves the manifold is homeomorphic to a sphere.

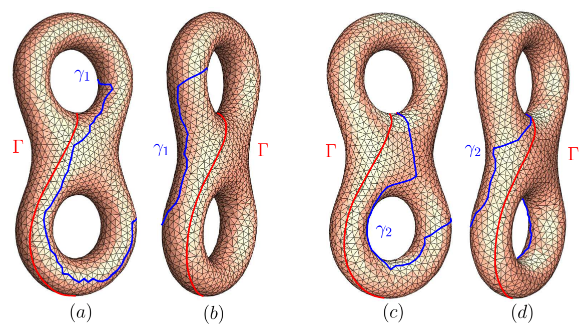

Fig. 1. Two homotopic closed surface γ_1 and γ_2 are given. The canonical representative of their homotopy class $[\gamma_1]$ is computed as the unique closed geodesic in the homotopy class under the uniformization metric, shown as Γ. (a) and (b) show the front view and back view of γ_1 and Γ. (c) and (d) illustrate the front view and back view of γ_2 and Γ. The figure shows the canonical representative of the homotopy class is unique.

In this work, we propose to assign a special Riemannian metric to a topological surface, which helps the computation for topological problems, especially those related to the fundamental group. The basic idea is that, each homotopy class has an infinite number of loops, if a unique representative can be selected from the loops, it can greatly simplifies the problems. A natural choice for the representative will be a closed geodesic. Unfortunately, under induced Euclidean metric, the closed geodesic is not unique in each homotopy class. According to Riemann uniformization theorem, each metric surface has a canonical uniformization metric, which has constant Gaussian curvature everywhere. If the surface is of negative Euler number, then under the canonical metric, each homotopy class has a unique closed geodesic. By deforming the metric to be the canonical uniformization metric, the unique closed geodesic can be obtained and used as the canonical representative for the class.

The major computational challenges are:

1) How to compute the uniformization metric?

2) How to compute the closed geodesic from a given loop?

The first problem can be solved using surface Ricci flow, which deforms the metric proportional to the Gaussian curvature, such that the curvature evolves according to a heat diffusion process, and becomes constant everywhere. This work introduces a novel discrete curvature flow, *discrete hyperbolic Yamabe flow on surfaces*, which is the gradient flow of a convex energy. The uniformization metric corresponds to the unique global optimum of the energy. By optimizing the energy, the optimum can be reached efficiently and stably.

The second problem can be solved using duality between the fundamental group and the Fuchsian group. The universal covering space of the surface can be isometrically embedded onto the hyperbolic space $\mathbb{H}^2$. All the deck transformations are Möbius transformations, and form the Fuchsian group. Each homotopy class corresponds to a unique Fuchsian transformation. The unique geodesic corresponds to the axis of the Fuchsian transformation.

The paper is organized in the following way: previous works are briefly reviewed in the next section; theoretic background is introduced in Section III; details for the algorithms are explained thoroughly in Sections IV and V; experimental results are reported in Section VI; the paper is concluded in Section VII.

2. PREVIOUS WORKS

The Ricci flow on surfaces The Ricci flow was firstly proposed by Hamilton [1] as a tool to conformally deform the metric according to the curvature. In [2] Chow and Luo developed the theories of the combinatorial surface Ricci flow, which was later implemented and applied for surface parameterization [3], [4], shape classification [5], shape mapping [6] and surface matching [7].

In [10] Luo studied the discrete Yamabe flow on surfaces. He introduced a notion of discrete conformal change of polyhedral metric, which plays a key role in developing the discrete Yamabe flow and the associated variational principle in the field. Based on the discrete conformal class and geometric consideration, Luo gave the discrete Yamabe energy as an integration of a differential 1-form and proved that this energy is a locally convex function. He also deduced from it that the curvature evolution of the Yamabe flow is a heat equation. In a very nice recent work of Springborn et al. [11] they were able to identify the Yamabe energy introduced by Luo with the Milnor-Lobachevsky function and the heat equation for the curvature evolution with the cotangent Laplace equation. They constructed an algorithm based on their explicit formula.

Theories of Yamabe flow on discrete hyperbolic surface can be found in [25]. This is the first work to develop the computational algorithm for *hyperbolic Yamabe flow*, which is used to compute the uniform hyperbolic metric for surfaces with negative Euler number.

The shortest loop The problem of computing homotopy geodesic, *homotopy class representative*, for loops or all point pairs has significant connections with other important problems in computational topology, such as constructing polygonal schema [12], [13], [14], contractibility test and transformability test [15].

Erickson and Whittlesey [16] gave a very fast greedy algorithm to compute the shortest system of loops relaxing the homotopy condition. The active contour method [17] is widely used in computer vision. A planar curve on an image can be shrunk by moving each point towards its curvature center. The deformation process does not change the homotopy type of the curve. Later, in [18], geometric snakes, which are cycles on a surface, are computed from active contours on the corresponding parameter chart. By distorting the curve based on geodesic curvature, the curves will be deformed to geodesics with the same homotopy type. Dey et al. [27] proposed the persistence based algorithm to compute well defined tunnel and handle base loops that are both topologically correct but also geometrically relevant. *handles and tunnels* are defined via homology. Thus it can not guarantee the loops detected are the representatives of homotopy group.

Hershberger and Soneyink lifted closed curves to the universal covering space in [20], [21]. However, their results only apply to boundary triangulated 2-manifolds and cannot be used in our case because it assumes all vertices are on a boundary. Yin et. al. [19] generalized the shortest path algorithm to the shortest cycles in each homotopy class on a surface with arbitrary topology, by utilizing the UCS in algebraic topology.

Jin et al. [22], [5], [26] introduced the geodesic spectra from Fuchsian group generators in a closed form to classify surfaces by their conformal structures. The key difference is that their method only computes the lengths of geodesics, which are the traces of the Fuchsian transformations. In our work, we focus on finding the geodesics explicitly, instead of just their lengths.

3. THEORETIC BACKGROUND

This section briefly introduces the theoretic background necessary for the current work. For details, we refer readers to [23] for algebraic topology and [24] for differential geometry.

Fundamental group and representative of homotopy class Let S be a topological surface, and let p be a point of S. All loops with base point p are classified by homotopy relation. All homotopy equivalence classes form the *homotopy group* or *fundamental group* $\pi_1(S,p)$, where the product is defined as the concatenation of two loops through their common base point.

Suppose S is a genus g closed surface. A *canonical set of generators* of $\pi(S,p)$ consists of $\{a_1,b_1,a_2,b_2,\cdots,a_g,b_g\}$, such that the pair a_i and b_i has one intersection point, the pairs $\{a_i,a_j\}$, $\{b_i,b_j\}$ and $\{a_i,b_j\}$, have no intersections, where $i \neq j$. See Figure 1 for an example of canonical basis on a genus two surface.

Universal cover and uniformization metric A *covering space* of S is a space $\tilde{S}$ together with a continuous surjective map $h : \tilde{S} \to S$, such that for every $p \in S$ there exists an open neighborhood U of p such that $h^{-1}(U)$ (the inverse image of U under h) is a disjoint union of open sets in $\tilde{S}$ each of which is mapped homeomorphically onto U by h. The map h is called the *covering map*. A simply connected covering space is a *universal cover*.

Suppose $\gamma \subset S$ is a loop through the base point p on S. Let $\tilde{p}_0 \in \tilde{S}$ be a preimage of the base point p, $\tilde{p}_0 \in h^{-1}(p)$, then there exists a unique path $\tilde{\gamma} \subset \tilde{S}$ lying over γ (i.e. $h(\tilde{\gamma}) = \gamma$) and $\tilde{\gamma}(0) = \tilde{p}_0$. $\tilde{\gamma}$ is a *lift* of γ.

A *deck transformation* of a cover $h : \tilde{S} \to S$ is a homeomorphism $f : \tilde{S} \to \tilde{S}$ such that $h \circ f = h$. All deck transformations form a group, the so-called *deck transformation group*. A *fundamental domain* of S is a simply connected domain, which intersects each orbit of the deck transformation group only once.

The deck transformation group $Deck(S)$ is isomorphic to the fundamental group $\pi_1(S,p)$. Let $\tilde{p}_0 \in h^{-1}(p)$, $\phi \in Deck(S)$, $\tilde{\gamma}$ is a path in the universal cover connecting $\tilde{p}_0$ and $\phi(\tilde{p}_0)$, then the projection of $\tilde{\gamma}$ is a loop on S, ϕ corresponds to the homotopy class of the loop, $\phi \to [h(\tilde{\gamma})]$. This gives the isomorphism between $Deck(S)$ and $\pi_1(S,p)$.

Surface Ricci curvature flow Let S be a surface embedded in $\mathbb{R}^3$. S has a Riemannian metric induced from the Euclidean metric of $\mathbb{R}^3$, denoted by $\mathbf{g}$. Suppose $u : S \to \mathbb{R}$ is a scalar function defined on S. It can be verified that $\bar{\mathbf{g}} = e^{2u}\mathbf{g}$ is also a Riemannian metric on S conformal to the original one.

The Gaussian curvatures will also be changed accordingly. The Gaussian curvature will become

$$\bar{K} = e^{-2u}(-\Delta_{\mathbf{g}} u + K),$$

where $\Delta_{\mathbf{g}}$ is the Laplacian-Beltrami operator under the original metric $\mathbf{g}$. The above equation is called the *Yamabe equation*. By solving the Yamabe equation, one can design a conformal metric $e^{2u}\mathbf{g}$ by a prescribed curvature $\bar{K}$.

Yamabe equation can be solved using *Ricci flow* method. The Ricci flow deforms the metric $\mathbf{g}(t)$ according to the Gaussian curvature $K(t)$ (induced by itself), where t is the time parameter

$$\frac{dg_{ij}(t)}{dt} = 2(\bar{K} - K(t))g_{ij}(t).$$

The *uniformization theorem* for surfaces says that any metric surface admits a Riemannian metric of constant Gaussian curvature, which is conformal to the original metric. Such metric is called the *uniformization metric*.

Poincaré disk model In this work, we use Poincaré disk to model the hyperbolic space $\mathbb{H}^2$, which is the unit disk $|z| < 1$ on the complex plane with the metric $ds^2 = \frac{4dzd\bar{z}}{(1-z\bar{z})^2}$. The rigid motion is the Möbius transformation

$$z \to e^{i\theta}\frac{z - z_0}{1 - \bar{z}_0 z},$$

where θ and z_0 are parameters. The geodesic of Poincaré disk is a Euclidean circular arc, which is perpendicular to the unit circle.

Suppose S is a high genus closed surface with the hyperbolic uniformization metric $\tilde{\mathbf{g}}$. Then its universal covering space $(\tilde{S}, \tilde{\mathbf{g}})$ can be isometrically embedded in $\mathbb{H}^2$. Any deck transformation of $\tilde{S}$ is a Möbius transformation, and called a *Fuchsian transformation*. The deck transformation group is called the *Fuchsian group* of S.

Let ϕ be a Fuchsian transformation, let $z \in \mathbb{H}^2$, the *attractor* and *repulser* of ϕ are $\lim_{n\to\infty}\phi^n(z)$ and $\lim_{n\to\infty}\phi^{-n}(z)$ respectively. The *axis* of ϕ is the unique geodesic through its attractor and repulser.

4. DISCRETE HYPERBOLIC YAMABE FLOW

In practice, most surfaces are approximated by discrete triangular meshes. Let M be a two dimensional simplicial complex, we denote the set of vertices, edges and faces as V, E, F respectively. We use v_i as the *ith* vertex; edge $[v_i, v_j]$ from v_i to v_j; face $[v_i, v_j, v_k]$ with the vertices sorted counter-clockwisely. Figure 2 shows the hyperbolic triangle, and its associated edge lengths l_i, y_i, corner angles θ_i and conformal factors u_i.

A *discrete metric* is a function $l : E \to \mathbb{R}^+$, such that triangle inequality holds on every face, which represents the edge lengths. In this work, we assume all faces are hyperbolic triangles. The *discrete curvature* $K : V \to \mathbb{R}$ is defined as angle deficit, 2π minus surrounding corner angles for an interior vertex, and π minus surrounding corner angles for a boundary vertex.

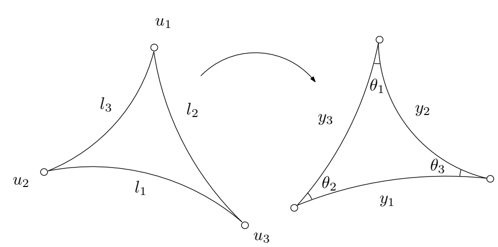

Fig. 2. Discrete surface Yamabe flow.

4.1 Discrete conformal deformation

Suppose the mesh is embedded in $\mathbb{R}^3$, therefore it has the induced Euclidean metric. We use l_{ij}^0 to denote the initial induced Euclidean metric on edge $[v_i, v_j]$.

Let $u : V \to \mathbb{R}$ be the *discrete conformal factor*. The discrete conformal metric deformation is defined as

$$\sinh(\frac{y_k}{2}) = e^{u_i}\sinh(\frac{l_k}{2})e^{u_j}. \quad (1)$$

The *discrete Yamabe flow* is defined as

$$\frac{du_i}{dt} = -K_i, \quad (2)$$

where K_i is the curvature at the vertex v_i.

Let $\mathbf{u} = (u_1, u_2, \cdots, u_n)$ be the conformal factor vector, where n is the number of vertices, $\mathbf{u_0} = (0, 0, \cdots, 0)$, then the *discrete hyperbolic Yamabe energy* is defined as

$$E(\mathbf{u}) = \int_{\mathbf{u_0}}^{\mathbf{u}} \sum_{i=1}^{n} K_i du_i. \qquad (3)$$

The following theorem lays down the foundation of the discrete hyperbolic flow algorithm.

Lemma IV.1. *The differential 1-form $\omega = \sum_{i=1}^{n} K_i du_i$ is closed.*

We use c_k to denote $\cosh(y_k)$. By direct computation, it can be shown that on each triangle,

$$\frac{\partial \theta_i}{\partial u_j} = A \frac{c_i + c_j - c_k - 1}{c_k + 1},$$

where

$$A = \frac{1}{\sin(\theta_k)\sinh(y_i)\sinh(y_j)},$$

which is symmetric in i, j, therefore $\frac{\partial \theta_i}{\partial u_j} = \frac{\partial \theta_j}{\partial u_i}$. It is easy to see that $\frac{\partial K_i}{\partial u_j} = \frac{\partial K_j}{\partial u_i}$, which implies $d\omega = 0$.

Theorem IV.2. *The discrete hyperbolic Yamabe energy is convex. The unique global minimum corresponding to the hyperbolic metric with zero vertex curvatures.*

This requires to compute the Hessian matrix of the energy. The explicit form is given as follows.

$$\frac{\partial \theta_i}{\partial u_i} = -A \frac{2c_i c_j c_k - c_j^2 - c_k^2 + c_i c_j + c_i c_k - c_j - c_k}{(c_j + 1)(c_k + 1)}$$

The Hessian matrix (h_{ij}) of the hyperbolic Yamabe energy can be computed explicitly. Let $[v_i, v_j]$ be an edge, connecting two faces $[v_i, v_j, v_k]$ and $[v_j, v_i, v_l]$, then the edge weight is defined as

$$h_{ij} = \frac{\partial \theta_i^{jk}}{\partial u_j} + \frac{\partial \theta_i^{lj}}{\partial u_j}.$$

also for

$$h_{ii} = \sum_{j,k} \frac{\partial \theta_i^{jk}}{\partial u_i},$$

where the summation goes through all faces surrounding v_i, $[v_i, v_j, v_k]$.

The discrete hyperbolic energy can be optimized using Newton's method directly. Because of the convexity of the energy, the optimization process is stable.

Given the mesh M, a conformal factor vector $\mathbf{u}$ is *admissible*, if the deformed metric satisfies triangle inequality on each face. The space of all admissible conformal factors is not convex. In practice, the step length in Newton's method needs to be adjusted. Once triangle inequality doesn't hold on a face, edge swap needs to be performed.

5. COMPUTATIONAL ALGORITHMS

The algorithm pipeline has two stages. The first stage is to compute the hyperbolic uniformization metric, the fundamental group generators and the corresponding Fuchsian group generators. This stage is independent of the input loop, and needs to be performed only once.

The second stage includes lifting the loop to the universal covering space (this can be accomplished symbolically without the real lifting process) to get the corresponding Fuchsian transformation; computing the axis of the Fuchsian transformation, and project the axis to the original surface.

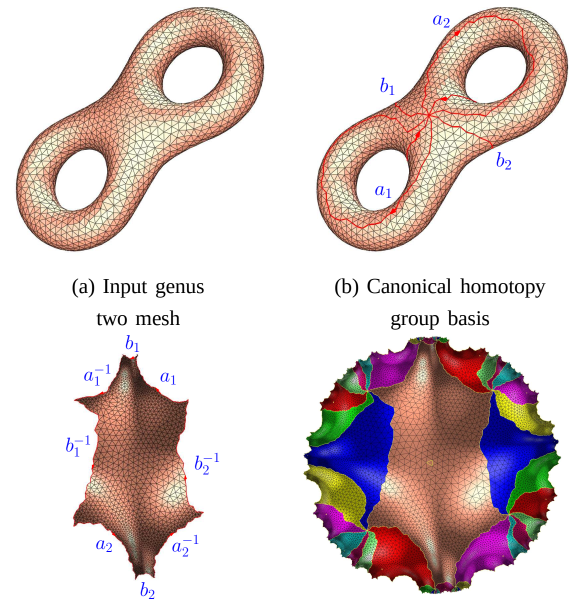

(a) Input genus two mesh

(b) Canonical homotopy group basis

(c) Fundamental domain embedded in $\mathbb{H}^2$ under hyperbolic metric

(d) Portion of universal covering space using Fuchsian group generators

Fig. 3. Algorithm pipeline: Stage 1. (a) is the input genus two mesh; (b) Compute a set of canonical fundamental group basis $\{a_1, b_1, a_2, b_2\}$; (c) Compute the hyperbolic uniformization metric using hyperbolic Yamabe flow. The fundamental domain is embedded onto $\mathbb{H}^2$ under the hyperbolic metric; (d) Compute the Fuchsian group generators. Any finite portion of the universal covering space can be constructed using these generators.

5.1 *Stage one*

Figure 3 illustrates the pipeline for the first stage. Suppose we are given a mesh with negative Euler number, as shown in frame (a).

1) Use hyperbolic Yamabe flow introduced in the last section to compute the hyperbolic metric, such that all vertex curvature equals to zero.
2) Compute a set of canonical fundamental group generators through a base vertex, as shown in frame (b). We use the method from Ericson [16]. We denote the generators as $\{a_1, b_1, a_2, b_2, \cdots, a_g, b_g\}$.
3) Slice the mesh M along the fundamental group generators to get an open mesh $\bar{M}$. The boundary of $\bar{M}$ is

$$\partial \bar{M} = a_1 b_1 a_1^{-1} b_1^{-1} \cdots a_g b_g a_g^{-1} b_g^{-1}.$$

Isometrically embed $\bar{M}$ onto the Poincaré disk using the hyperbolic uniformization metric to get a fundamental domain, still denoted as $\bar{M}$. As shown in frame (c). The embedding method is similar to that in [4].

4) Compute the Fuchsian group generators corresponding to the fundamental group generators. Let γ be a fundamental group generator. Because $\bar{M}$ has been embedded onto the Poincaré disk, $\gamma \in \partial\bar{M}$, we treat γ as a curve segment on the Poincaré disk. We compute the unique Fuchsian transformation ϕ, such that ϕ maps γ^{-1} to γ. First a Möbius transformation can be calculated such that the starting vertex of γ is mapped to the origin, the ending vertex is mapped to a positive real number. Similarly we find another Möbius transformation for γ^{-1}. The composition of the second map with the inverse of the first map is the desired Fuchsian transformation. We denote the Fuchsian transformations as α_i corresponding to a_i, β_j corresponding to b_j.

5.2 *Stage two*

Suppose a loop is given on the surface, denoted as γ. The following pipeline explains how to find the closed geodesic Γ homotopic to γ. Figures 4 and 5 illustrate two key steps: (1) loop lifting and (2) geodesic tracing.

1) Perturbable γ to make it transverse all the fundamental group generators. As shown in frame (a) and (b).
2) Choose a vertex $v \in \gamma$, trace γ. Once γ across a fundamental group generator, record the Id of the generator. After tracing back to the starting vertex v, a word is obtained. $w = \sigma_1\sigma_2\cdots\sigma_k$, where $\sigma_i(1 \le i \le k)$ is in $\{a_1, b_1, a_1^{-1}, b_1^{-1}, \cdots, a_g, b_g, a_g^{-1}, b_g^{-1}\}$.
3) Convert the word w to
$$\phi = \phi_k \circ \phi_{k-1} \cdots \phi_2 \circ \phi_1,$$
where $\phi_i(1 \le i \le k)$ is the Fuchsian transformation corresponding to σ_i.
4) Lift γ to $\tilde{\gamma}$ in the universal covering space, called **loop lifting**. Start from $\bar{M}$, trace γ on S and extend $\tilde{\gamma}$ on $\tilde{S}$ accordingly. Once γ crosses σ_k, transform the current fundamental domain by ϕ_k, continue the tracing on the new fundamental domain. As shown in Figure 4, a loop γ intersects the fundamental group generators in the order of $w = \{a_2^{-1}, a_2^{-1}, b_2, a_1^{-1}, a_1^{-1}, b_1\}$. γ is lifted to Γ in the universal covering space, in frame (c) Γ crosses the fundamental domain through a_2^{-1}. In the followings frames, Γ crosses different fundamental domains. The whole lifted Γ is shown in frame (j). This step can be omitted in practice, only the word of intersection w is needed.
5) Compute the axis of ϕ. First compute the attractor and repulser of ϕ, then determine the unique geodesic through them. Denote the axis as $\tilde{\Gamma}$.
6) Trace $\tilde{\Gamma}$ from the central fundamental domain $\bar{M}$, called **geodesic tracing**. Once Γ crosses the boundary of the current fundamental domain, find the Fuchsian transformation ϕ_k corresponding the boundary segment, transform the current fundamental domain by ϕ_k, and continue the tracing on the new fundamental domain. At the same time, during the tracing, project $\tilde{\Gamma}$ to the original surface, denoted as Γ. If Γ becomes a smooth closed loop, stop tracing. Then Γ is the canonical representative for the homotopy class $[\gamma]$. As shown in Figure 5, frame (c) to (i) illustrate the tracing process. Frame (j) shows the tracing result of the geodesic. Frame (a) and (b) show the geodesic on the original surface, which is the canonical representative of the homotopy class $[\gamma]$.

TABLE 1
COMPUTATIONAL TIME.

Figure	Model	Genus	Faces	Vertices	Time (s)
Fig. 3	2-hole	2	4118	2057	13
Fig. 6	Amaphora	2	20010	10003	107
Fig. 7	Knotty	2	10000	6066	36
Fig. 8	3-hole	3	3514	1754	12
Fig. 9	3-torus	3	16000	8002	87

6. EXPERIMENT RESULTS

We implement our algorithm using generic C++ on a Windows platform. The experiments are conducted on a desktop with 2.33 GHz dual CPU and 3.98GB RAM.

The surfaces are represented as triangle meshes using half-edge data structure. We apply Newton's method for optimizing the discrete hyperbolic Yamabe energy, which involves solving large sparse linear system. We use Matlab C++ library for the numerical computation. The computational time on test data is reported in Table 1. Figures 3, 6, 7, 8 and 9 show the hyperbolic metric using the hyperbolic Yamabe flow method. Table 2 illustrates the exact values for corresponding Fuchsian group generators.

Figures 1, 4 and 5 show the results on a two-hole model, which has $16,472$ triangles and $8,234$ vertices. The algorithm takes 13 seconds to compute the hyperbolic metric with error bound $\varepsilon = 1e-10$, and takes 1 second for the rest. The timing is reported in the table.

We apply our algorithm for detecting whether two loops are homotopic as shown in Figure 1 and Figure 5. The initial loops and their unique homotopy representatives are illustrated in front and back views respectively. We can see that the representatives are not identical, therefore, the loops are not homotopic.

Figures 10, 11 and 12 give the results on a three-hole model, which has $3,514$ triangles and $1,754$ vertices. The algorithm takes 12seconds to compute the hyperbolic metric with error bound $\varepsilon = 1e-10$, and takes 1 second for the rest.

7. CONCLUSION

This paper introduces a method to compute the canonical representative for each homotopy class based on hyperbolic structure of the surface. A novel curvature flow is introduced, discrete hyperbolic Yamabe flow, which

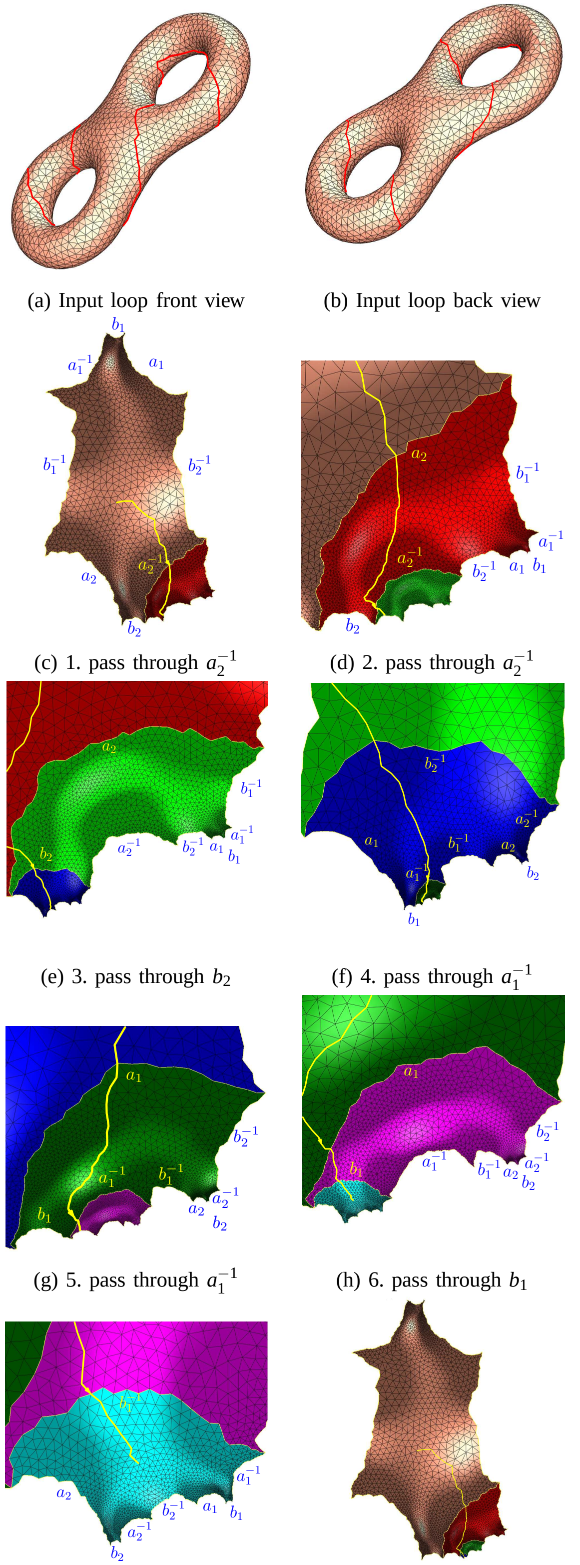

(a) Input loop front view (b) Input loop back view (c) 1. pass through a_2^{-1} (d) 2. pass through a_2^{-1} (e) 3. pass through b_2 (f) 4. pass through a_1^{-1} (g) 5. pass through a_1^{-1} (h) 6. pass through b_1 (i) Final ending (j) Whole lift in $\mathbb{H}^2$

Fig. 4. Algorithm pipeline: Stage 2. Loop lifting. A loop γ intersects the fundamental group generators in the order of $w = \{a_2^{-1}, a_2^{-1}, b_2, a_1^{-1}, a_1^{-1}, b_1\}$. γ is lifted to Γ in the universal covering space. (c) to (i) illustrate that Γ crosses the fundamental domain through a_2^{-1},a_2^{-1},b_2,a_1^{-1},a_1^{-1} and b_1 orderly. (j) the lifting result of loop Γ.

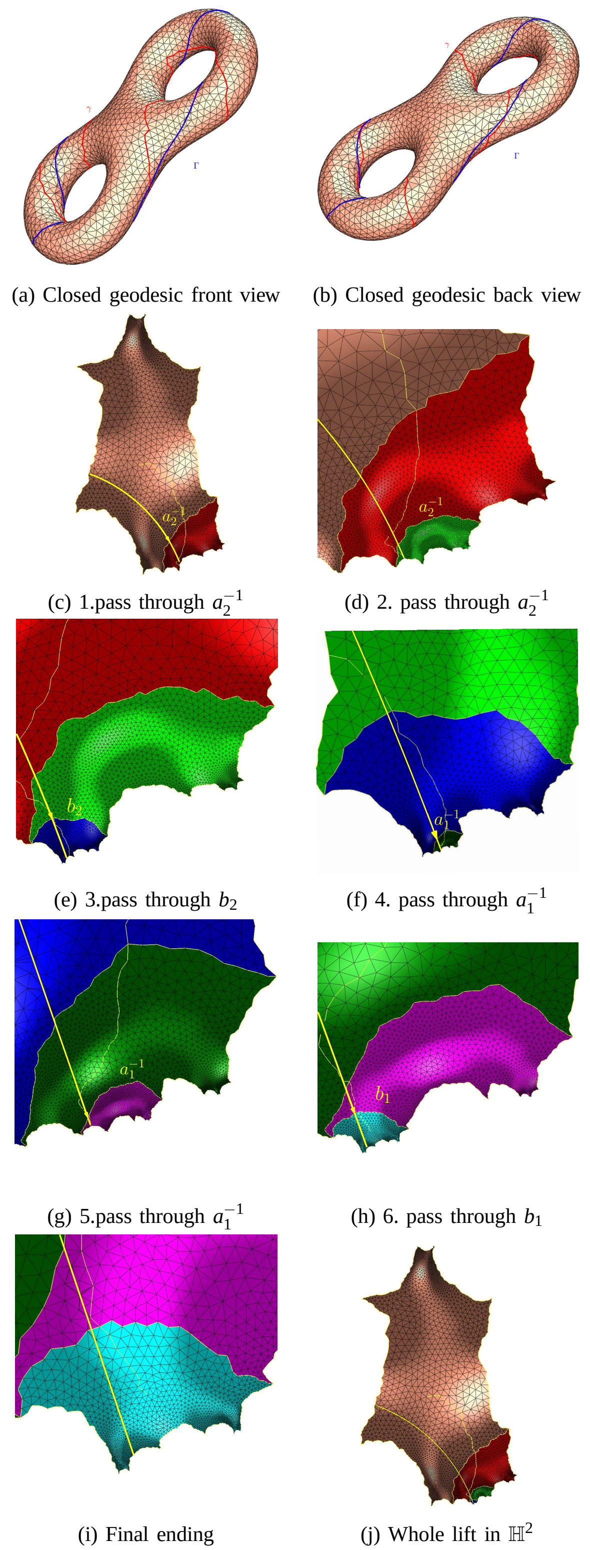

(a) Closed geodesic front view (b) Closed geodesic back view (c) 1.pass through a_2^{-1} (d) 2. pass through a_2^{-1} (e) 3.pass through b_2 (f) 4. pass through a_1^{-1} (g) 5.pass through a_1^{-1} (h) 6. pass through b_1 (i) Final ending (j) Whole lift in $\mathbb{H}^2$

Fig. 5. Algorithm pipeline: Stage 2. Geodesic tracing. (a) and (b) the geodesic on the original surface, which is the canonical representative of the homotopy class $[\gamma]$. (c) to (i) illustrate the tracing process. (j) the tracing result of the geodesic.

is the gradient flow of Yamabe energy. The convexity of Yamabe energy grantees the convergence of the flow and the uniqueness of the solution. The geodesic is computed as the axis of the Fuchsian transformation corresponding to the given homotopy class.

The algorithm is explained in details by illustrations.

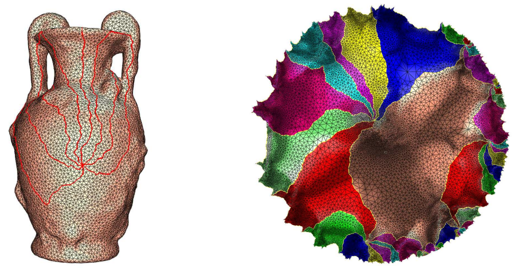

(a) Fundamental group generators (b) Universal covering space

Fig. 6. Hyperbolic metric and the Fuchsian group generators for the Amphora model.

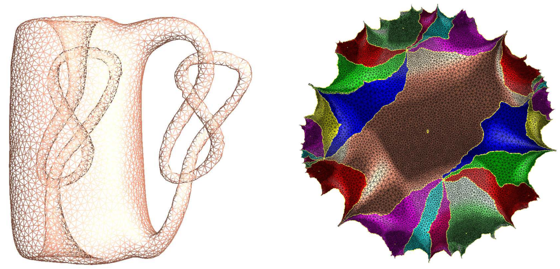

(a) Fundamental group generators (b) Universal covering space

Fig. 7. Hyperbolic metric and the Fuchsian group generators for the Knotty model.

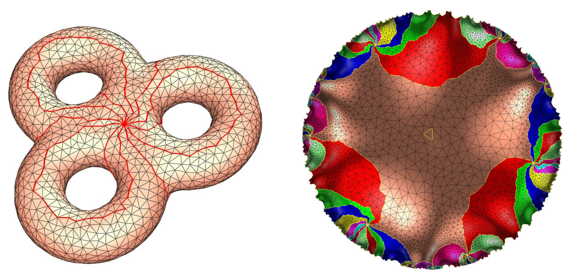

(a) Fundamental group generators (b) Universal covering space

Fig. 8. Hyperbolic metric and the Fuchsian group generators for the 3-hole model.

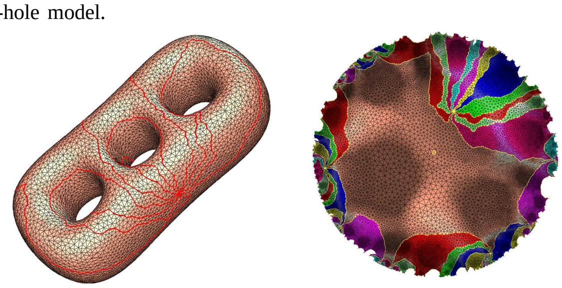

(a) Fundamental group generators (b) Universal covering space

Fig. 9. Hyperbolic metric and the Fuchsian group generators for the 3-torus model.

The efficiency and efficacy of the algorithm is demonstrated by various experiments on high genus surfaces.

There are many potential applications, such as finding the shortest word for a homotopy class in the fundamental group; shape comparison; canonical surface segmentation etc. The whole method can be generalized to discrete 3-manifolds directly. In the future, we will explore along these directions.

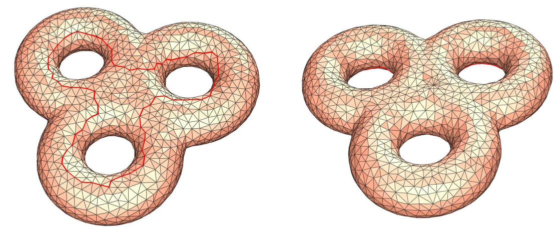

(a) Front view (b) Back view

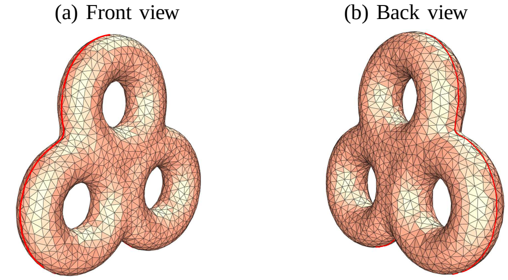

(c) Left view (d) Right view

Fig. 10. Homotopy geodesic on 3-hole torus 1.

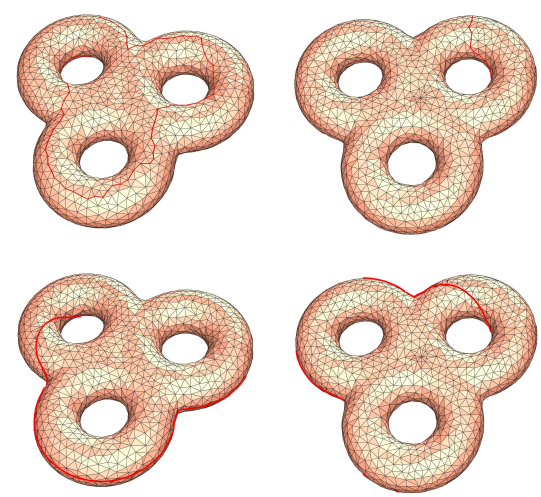

(a) Front view (b) Back view

Fig. 11. Homotopy geodesic on 3-hole torus 2.

ACKNOWLEDGMENTS

This work is partially supported NSF CCF-0448399, DMS-0528363, DMS-0626223 and NSFC-60628202.

REFERENCES

[1] R. S. Hamilton, Three manifolds with positive Ricci curvature, Journal of Differential Geometry, 1982, 17: 255-306.

[2] B. Chow and F. Luo, Combinatorial ricci flows on surfaces, Journal Differential Geometry 2003, 63(1): 97-129.

[3] M. Jin, F. Luo and X. Gu. Computing surface hyperbolic structure and real projective structure, SPM '06: Proceedings of the 2006 ACM Symposium on Solid and Physical Modeling, 2006: 105-116.

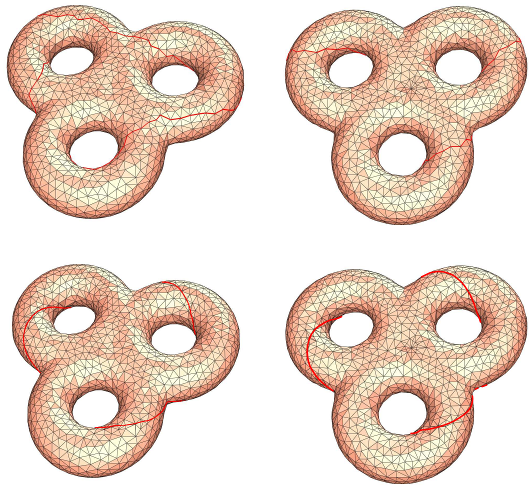

(a) Front view (b) Back view

Fig. 12. Homotopy geodesic on 3-hole torus 3.

TABLE 2
FUCHSIAN GENERATORS.

Model	Generator	z_0.*real*	z_0.*imag*	θ
Fig. 5 2-hole	a_1	0.830937	0.419568	2.26744
	b_1	0.0785149	0.96558	1.67718
	a_2	-0.703859	-0.54534	2.03098
	b_2	0.186691	-0.943763	1.48676

Model	Generator	z_0.*real*	z_0.*imag*	θ
Fig. 6 Amphora	a_1	0.478882	-0.836208	2.00886
	b_1	0.855238	-0.204422	1.74862
	a_2	-0.870138	-0.416603	1.91529
	b_2	-0.796646	-0.579835	2.69912

Model	Generator	z_0.*real*	z_0.*imag*	θ
Fig. 7 Knotty	a_1	0.892765	-0.26021	2.38572
	b_1	0.38619	0.921787	1.30992
	a_2	-0.852484	0.260488	2.1975
	b_2	-0.129811	-0.990796	0.93043

Model	Generator	z_0.*real*	z_0.*imag*	θ
Fig. 8 3-hole	a_1	-0.977168	0.092502	1.99611
	b_1	-0.961125	-0.184911	2.57482
	a_2	0.493651	-0.840193	1.74765
	b_2	0.743817	-0.622356	2.4617
	a_3	0.408767	0.888353	1.876
	b_3	0.143125	0.967503	2.56559

Model	Generator	z_0.*real*	z_0.*imag*	θ
Fig. 9 3-torus	a_1	-0.451831	-0.833918	1.92286
	b_1	0.272943	-0.89847	1.84151
	a_2	0.665799	0.729522	2.57521
	b_2	0.606916	0.792085	2.90907
	a_3	-0.674179	0.689653	1.96083
	b_3	-0.910911	0.39714	2.43426

[4] M. Jin, J. Kim, F. Luo, and X. Gu. Discrete surface ricci flow, IEEE TVCG 2008, 14(5): 1030-1043.
[5] M. Jin, W. Zeng, F. Luo and X. Gu, Computing Tëichmuller Shape Space, IEEE TVCG 2008, 99(2): 1030-1043.
[6] X. Li, Y. Bao, X. Guo, M. Jin, X. Gu and H. Qin. Globally Optimal Surface Mapping for Surfaces with Arbitrary Topology, IEEE Transactions on Visualization and Computer Graphics, 2008, 14(4): 805-819.
[7] W. Zeng, X. Yin, Y. Zeng, Y. Wang, X. Gu, and D. Samaras, 3D Face Matching and Registration Based on Hyperbolic Ricci Flow. In CVPR 2008 Workshop on 3D Face Processing, 2008.
[8] F. Luo, X. Gu and J. Dai, Variational Principles for Discrete Surfaces, Advanced Lectures in Mathematics, Vol.4, International Press of Boston, August 2008.
[9] M. Jin, F. Luo and X. Gu. Computing general geometric structures on surfaces using Ricci flow. Computer-Aided Design 2007, 39(8): 663-675.
[10] Feng Luo. Combinatorial yamabe flow on surfaces. Commun. Contemp. Math., 6(5):765-780, 2004.
[11] Boris Springborn, Peter Schröder, and Ulrich Pinkall. Conformal equivalence of triangle meshes. ACM Transactions on Graphics 2008, 27(3): 1-11.
[12] G. Vegter and C. Yap. Computational complexity of combinatorial surfaces. In Proceedings of the 6th ACM Symposium on Computational Geometry, 1990: 102-111.
[13] H. Schipper. Determining contractiblity of curves. In Proceedings of the 8th ACM Symposium on Computational Geometry, 1992: 358-367.
[14] T. K. Dey and H. Schipper. A new technique to compute polygonal schema for 2-manifolds with application to nullhomotopy detection. Discrete and Computational Geometry 1995, 14: 93-110.
[15] T. K. Dey and S. Guha. Transforming curves on surfaces. Journal of Computer and System Sciences 1999, 58: 297-325.
[16] J. Erickson and K. Whittlesey, Greedy optimal homotopy and homology generators. In: SODA 2005: 1038-1046.
[17] M. Kass, A. Witkin, and D. Terzopoulos. Snakes: Active contour models. In International Journal of Computer Vision 1988: 321-331.
[18] Y. Lee and S. Lee. Geometric snakes for triangular meshes. Computer Graphics Forum at Eurographics 2002, 21(3): 229-238.
[19] X. Yin, M. Jin and X. Gu. Computing Shortest Cycles Using Universal Covering Space, Computer-Aided Design and Computer Graphics, 2007 10th IEEE International Conference.
[20] J. Hersberger and J. Snoeyink. Around and around: computing the shortest loop. In Proceedings of the third Canadian Conference on Computational Geometry, 1991: 157-161.
[21] J. Hersberger and J. Snoeyink. Computing minimum length paths of a given homotopy class. In Proceedings of the second Workshop on Algorithms and Data Structures, 1991.
[22] M. Jin, F. Luo, S. Yau, X. Gu. Computing geodesic spectra of surfaces, In SPM 2007: 387-393.
[23] J. R.Munkres. Elements of algebraic topology. Addison-Wesley Co., 1984.
[24] Richard Schoen, Shing-Tung Yau. Lectures on differential geometry, International Press of Boston, 1994.
[25] A. Bobenko, B. Springborn, U. Pinkall. Discrete conformal equivalence and ideal hyperbolic polyhedra. In preparation.
[26] M.Jin, W.Zeng, X.Gu. Computing Fenchel-Nielsen Coordinates in Teichm "uller Shape Space, In SMI 2009.
[27] T. K. Dey, K. Li, J. Sun, D. Cohen-Steiner. Computing geometry-aware handle and tunnel loops in 3D models, ACM Trans. Graph., 27(3), 2008